Journal of the European Ceramic Society 22 (2002) 143–152

www.elsevier.com/locate/jeurceramsoc

Elaboration of low shrinkage mullite by active filler controlled pyrolysis of siloxanes

Thibaut Michalet [a], Michel Parlier [a], Franck Beclin [b], Richard Duclos [b], Jacques Crampon [b,*]

[a] *Office National d'Etudes et de Recherches Aérospatiales, DMSC, 92322 Châtillon, France*
[b] *Laboratoire de Structure et Propriétés de l'Etat Solide, ESA-CNRS 8008, Université des Sciences et Technologies de Lille, Bât. C6, 59655 Villeneuve d'Ascq, France*

Received 28 October 2000; received in revised form 19 February 2001; accepted 23 February 2001

Abstract

The active filler controlled pyrolysis of polymers has been used to synthesize mullite from Al_2O_3-filled, Al-filled and Al/Al_2O_3-filled siloxanes. Due to the presence of transition alumina and to a finer scale of mixing of the mullite precursors provided from active Al-filler, the beginning of mullitization temperature was lowered in the two last systems (1200–1250°C) in comparison to the first one (1400°C). The mullite equiaxed-grains obtained from the polymer/Al_2O_3 (PAO) system contained a large amount of dislocations whereas in polymer/Al (PA) and polymer/Al/Al_2O_3 (PAAO) derived samples they were primarily dislocation free. The presence of small amounts of residual glassy phase was observed as glassy pockets at triple-junctions in the whole of the materials. The improved microstructure obtained with the Al/Al_2O_3-filled mixture indicates that this system seems to be a good choice for a low shrinkage and low defect mullite, in comparison to mullite obtained from Al-filled and Al_2O_3-filled siloxanes.

Keywords: AFCOP; Al_2O_3; Mullite; Precursors-organic; Siloxane; Sintering

1. Introduction

The application of ceramic composites in aircraft engines requires long term and high temperature (above 1000°C) stability in an oxidizing atmosphere. Oxide–oxide ceramic composites are promising candidates because of their inherent stability in air at high temperature.[1] They can play an alternative to the super-alloys.[2–4] The fabrication of composite ceramics via sintering of ceramic powders requires two conditions: first, the matrix shrinkage during sintering must be limited, and second, in order to preserve the fibre integrity, relatively low sintering temperature must be used. Recently, the formation of monolithic and composite structural ceramics, by the reaction-bonding process, using ceramic and metallic powder mixtures, has been reported. The application of this process to alumina permits to obtain high density monoliths with a strongly limited shrinkage.[5–9] Nevertheless, in the case of the composite synthesis, the reaction-bonding process has some limitations (e.g. the infiltration of the powder in a fibrous preform is difficult).

At the same time, several authors have developed the composite synthesis from organo-metallic precursors. Used at first for the synthesis of SiC-based fibres,[10] the ceramic polymeric precursors have been also applied to the synthesis of monoliths of Si–C–O, SiC or Si_3N_4.[11–13] Nevertheless, the most important drawbacks of the method are the large shrinkage together with the polymer degradation during the pyrolysis, responsible for the monolith cracking. In the last 10 years, numerous searches have been devoted to the ceramic synthesis via filled polymers (active filler controlled polymer pyrolysis). The filler, identical to a 'skeleton' may react with the product of the polymer pyrolysis, and thus, limit the shrinkage.[14–17]

The advantages of this method when applied to mullite are : (i) possibility of complex shapes, (ii) improvement of the homogeneity, (iii) moderate processing temperature due to the high reactivity of amorphous

* Corresponding author.
E-mail address: jacques.crampon@univ-lille1.fr (J. Crampon).

0955-2219/01/$ - see front matter
PII: S0955-2219(01)00251-5

silica (SiO_2) yielded by the polymer precursor.[18–20] In this contribution, mullite monoliths are processed, associating the pyrolysis of the silica polymer precursor with Al_2O_3 powder and/or with the reaction-bonding of Al powder. The processed monoliths are characterised by thermal analysis, X-ray diffraction (XRD), Hg porosimetry and electron microscopy. The behaviour of the polymer/Al_2O_3 (PAO) mixture is compared with those of polymer/Al and polymer/Al/Al_2O_3 (PAAO) mixtures.

2. Experimental

A commercial solid polydimethylsiloxane (NH2000, Hüls, Germany) was used as a silica precursor. Chemical analysis of the polymer is listed in Table 1. Aluminium (A1183, Cerac, USA) and α-Al_2O_3 (CR1-AS1, 500 wt-ppm MgO-doped alumina, Baikowski chimie, France) with a median particle size of 0.8 and 1 μm, respectively, were used as filler components. Chemical impurities in aluminium and alumina are listed in Tables 2 and 3.

By variation of the content of Al and α-Al_2O_3, respectively, suitable polymer/filler ratios, with respect to stoichiometric 3/2 mullite, were determined for the three compositions: polymer/α-Al_2O_3 (PAO), polymer/Al (PA) and polymer/Al/ α-Al_2O_3 (PAAO) (Table 4).

Powder mixtures were processed in organic medium (propanol-2/acetone, 75/25 vol.%) with magnetic and ultrasonic homogenisation. After evaporating the solvent at 60°C, the residue was granulated through a 100 μm sieve, and then uniaxially pressed (15 MPa, 130°C) to yield solid samples of 90×16×4 mm with low residual porosity (3–7%). The heat-treatment of the samples was performed at temperatures up to 1550°C (3 h) with heating rates in the range 1–5°C/min in conventional electric furnaces. The first stage of heat-treatment was the pyrolysis of the polymer with an isothermal hold at 700°C (2 h) for oxidation of the polymer into SiO_2. The second stage was reaction sintering with an additional soaking time at 1100°C (2 h) to oxidize Al into alumina, when using this metal directly as a filler component.

Differential thermal analysis, thermogravimetric analysis (DTA/TGA) and dilatometry were used during the reaction to monitor, up to 1550°C, the associated phase, mass and dimension changes respectively. The porosity was characterized by Hg porosimetry. Reaction products, present between 1100 and 1550°C, were identified at room temperature by XRD patterns of crushed samples, using monochromatic Cu K_α radiation.

Microstructure of the sintered samples was examined by scanning electron microscopy (SEM) using polished and then thermally etched surfaces. Specimens for transmission electron microscopy (TEM) and for analytical transmission electron microscopy investigations (ATEM, Philips CM30 operating at 300 kV) using an attached energy dispersive X-ray spectrometer (EDS) were ion-thinned with a 5 kV argon beam. The EDS spectrometer has an ultra-thin window which allows the detection and quantification of oxygen. The method used for the thickness determination of the analysed area was based on the electrical neutrality condition.

Table 1
Silica precursor polymer composition (NH2000, Hüls)

	Si	C	H	O	Na	Cl	K	Ca
wt.%	38.25	15.39	5.2	41.16	–	–	–	–
wt-ppm	–	–	–	–	85	20	54	209

Table 2
Impurities in aluminium powder (A1183, Cerac)

	Fe	Si	Mg	Ca	Ti	V	Cr	Mn
wt-ppm	2000	1000	100	100	100	100	100	100

Table 3
Impurities in alumina powder (CR1-AS1, Baikowski chimie)

	Na	Mg	Si	Ca	Fe
wt-ppm	200	400	200	100	63

Table 4
Polymer/filler ratios for the three composition

Specimen	wt.%	vol.%
NH 2OOO/α-Al_2O_3 (PAO)	32.5/67.5	59/41
NH 2OOO/Al (PA)	47.5/52.5	65/35
NH 2OOO/Al/α-Al_2O_3 (PAAO)	39.5/24.5/36	62/19/19

3. Results and discussion

3.1. Thermoanalytical characterisation

The oxidation sequences of PAO system are fully similar to those of the polydimethylsiloxane alone. The specific mass change (TGA) in air (Fig. 1) shows that degradation and thermal oxidation of the polymer start at temperatures above 200°C and are completed at 800°C. The weight loss, −5.5%, is only due to the pyrolysis converting the polymer into silica. The differential thermal analysis (DTA) signal presents two exothermic peaks, at 260 and 520°C respectively, indicating that oxidation of the methyl groups follows a two-step sequence. Studies of similar polydimethylsiloxane have shown that, in the first temperature range 150–390°C, the Si–CH_3 bonds are broken, which results in the formation of transient peroxy and hydroperoxy radicals. In the second range, around 435°C, the subsequent oxidation of these radicals yields amorphous SiO_2.[21]

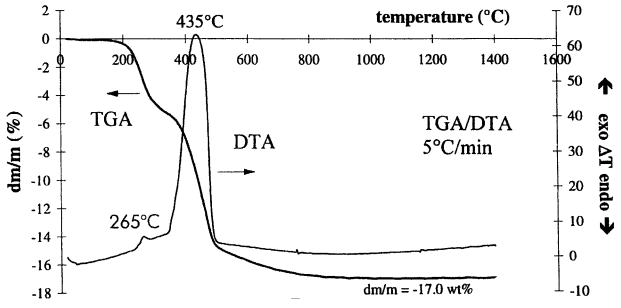

Fig. 1. TGA and DTA curves of polydimethylsiloxane (TGA/DTA 5°C min^{-1}).

In the case of PAAO and PA mixtures, the reaction steps are significantly different (Fig. 2). The weight loss due to the thermal degradation of the polymer is progressively compensated, between 300 and 500°C, by a mass increase due to the beginning of the oxidation of Al, in solid state, into alumina. The two exothermic peaks of the differential thermal analysis (DTA), characteristic of the degradation/thermal oxidation of the polymer, appear, at about 280–290 and 550°C, respectively. The observed temperature offset, in comparison with the PAO sample (260 and 520°C, respectively), is in relation with the subsequent oxidation of Al into Al_2O_3. A sharp exothermic peak at about 600°C shows clearly the oxidation process of solid Al particles. After a soaking time at 700°C (2 h), the process accelerates with another oxidation exothermic peak at 830°C. The rupture of the oxide scale due to the thermal expansion of the melt results in a rapid oxidation of Al, in the liquid state, into Al_2O_3.[7] The weak endothermic peak at 660°C corresponds effectively to the melting of Al metal. Another endothermic peak appears at 1410°C and is attributed to the melting of free Si metal. This peak is absent in the case of the polymer/Al_2O_3 system and thus, the presence of free Si in the PAAO and PA systems at high temperature can be correlated to the consumption of the oxygen from the polymer by the oxidation of Al.

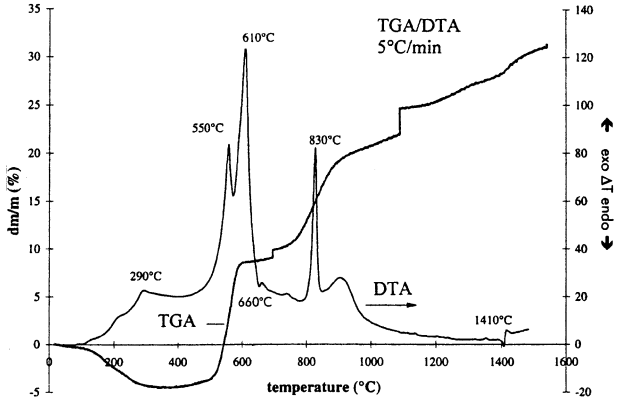

Fig. 2. TGA and DTA curves of polydimethylsiloxane/Al mixture (TGA/DTA 5°C min^{-1}).

Indeed, energetically it appears more favourable to oxidize Al rather than Si, as the oxidation reactions (1) and (2), with $\Delta G_I > \Delta G_{II}$,[22] show.

$$\text{I}\quad O_2(g) + 4/3Al = 2/3Al_2O_3(s) - \Delta G_I \tag{1}$$

$$\text{II}\quad O_2(g) + Si = SiO_2(s) - \Delta G_{II} \tag{2}$$

3.2. Phase development

The phase evolution for the PAO system as determined by XRD is shown in Fig. 3. The only crystalline phase present in the PAO microcomposite at 700°C, is α-Al_2O_3. No phase reaction is observed up to 1200°C, only the α-Al_2O_3 is identified and the small diffuse hump, in the $2\theta = 20°$ range, indicates the presence of amorphous silica. Amorphous silica crystallizes above 1250°C into some small amount of cristobalite that can be clearly identified in addition to α-Al_2O_3 by an intense XRD peak showing its maximum at 1350°C. Initial mullitization is

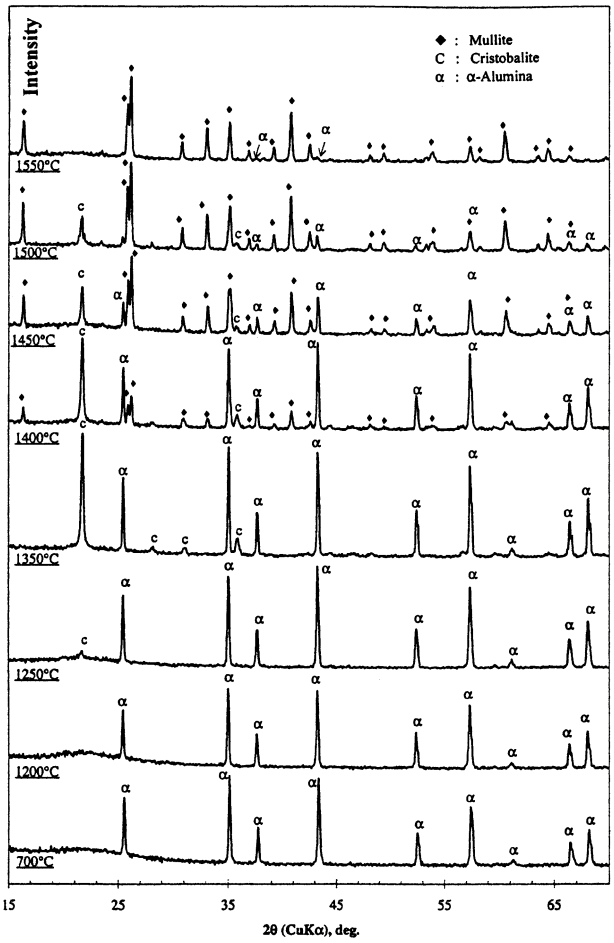

Fig. 3. X-ray diffraction patterns of the PAO system; phase evolution during heat treatment.

only detected at 1400°C after the extensive crystallization of amorphous SiO_2 into cristobalite. At 1450°C, three phases are coexisting : α-Al_2O_3 and cristobalite, that are still present, and mullite whose formation is enhanced. Between 1450 and 1550°C, together with mullite formation, the amount of α-Al_2O_3 and cristobalite progressively disappears. Finally at 1550°C PAO sample consists mainly of 3/2 mullite, with traces of α-Al_2O_3.

The evolution of the reactions in the case of siloxane/Al compounds is shown in Fig. 4. The XRD pattern at 700°C yields γ-Al_2O_3 as the only new crystalline phase, coexisting with the Al metal. Here again, the relatively high background is attributed to the presence of amorphous silica. After heat treatment up to 1200°C, the oxidation of the composite results in the formation of new transition alumina polymorphs (θ and δ phases are presumably present) together with a small amount of the stable α-Al_2O_3 phase and free Si. At 1250°C, PA composite begins to mullitize with the consumption of transition alumina. At 1300°C, the extent of mullite formation increases while the extensive crystallization of amorphous SiO_2 into cristobalite occurs. The mullite coexists with α-Al_2O_3 and cristobalite from 1300 up to 1500°C. This temperature range is somewhat lower than that for the PAO sample, which presents nearly the same pattern in the temperature range 1400–1500°C. The subsequent annealing behaviour is comparable to that of the siloxane/Al_2O_3 system, and also yields a 3/2 mullite with, in this case, apparently no excess alumina (1550°C, 3 h). Here, the presence of free Si in the XRD patterns is noted at a temperature up to 1350°C, which confirms the endothermic peak in DTA analysis at 1410°C.

The development of crystalline phases from the PAAO mixture on heating is shown in the corresponding XRD diagrams in Fig. 5. The pattern at 700°C yields γ-Al_2O_3 as the only new crystalline phase, coexisting with α-Al_2O_3 and the Al metal. After 3 h at 1100°C, the present phases are α-Al_2O_3, an amorphous phase (identified by a broad peak at around $2\theta = 20°$), traces of transition alumina (γ, θ and δ) and free Si. After 3 h at 1200°C, the mullitization takes place along with the beginning of the crystallization of cristobalite. At 1250°C the crystallization of cristobalite shows a maximum. At 1300°C, due to the consumption of transition alumina with mullite formation, only the stable α-

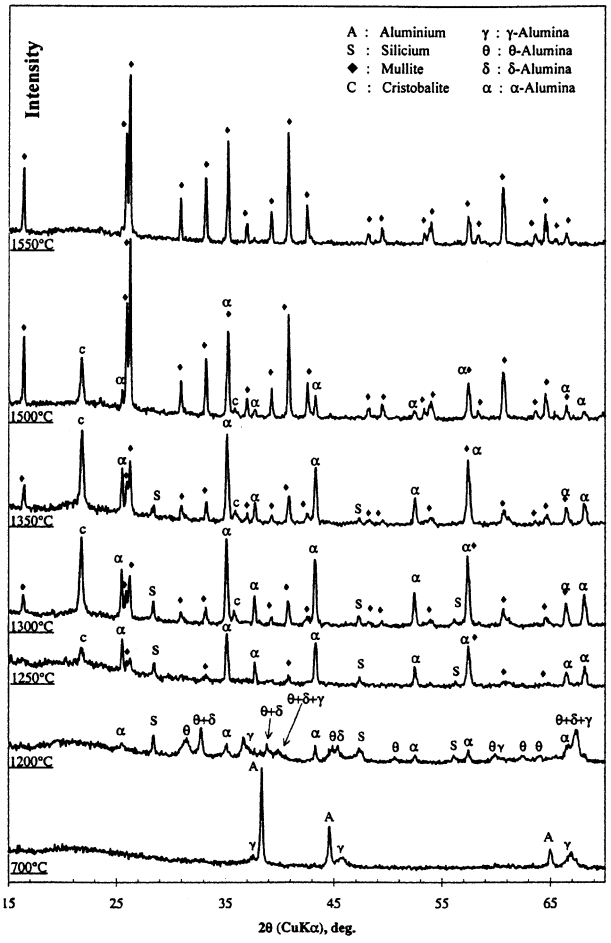

Fig. 4. X-ray diffraction patterns of the PA system; phase evolution during heat treatment.

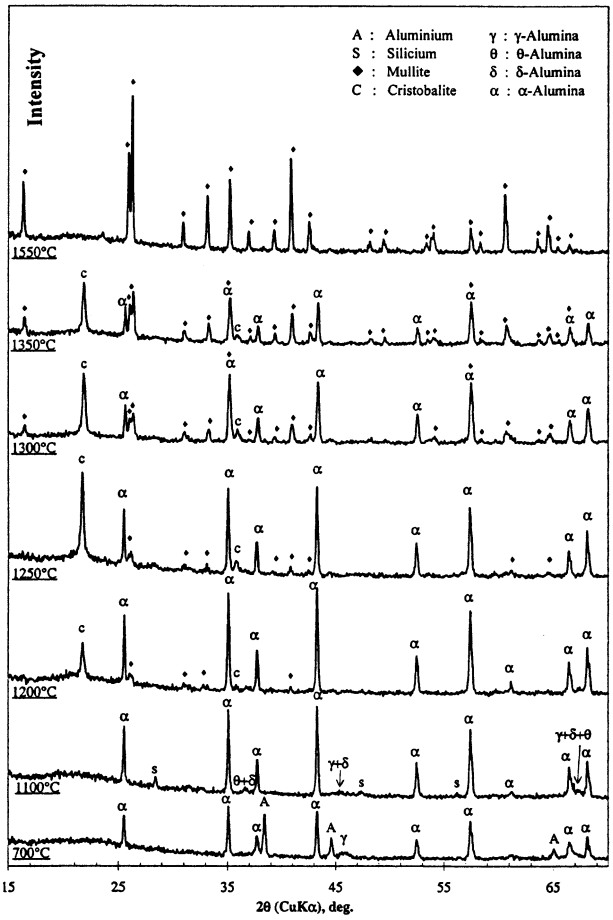

Fig. 5. X-ray diffraction patterns of the PAAO system; phase evolution during heat treatment.

phase is still present as a source of alumina. On further heating to 1550°C for 3 h, the main crystalline phase present is 3/2 mullite as in the case of the PAO and PA systems.

Mullite formation temperature and rate during reaction sintering of alumina–silica mixtures depend on various parameters. The most important of them are the nature (colloidal, amorphous or crystalline) of the source of the SiO_2 molecules,[23] the presence or absence of α-Al_2O_3 as the source of the Al_2O_3 molecules,[23] the particle size[24] and the scale of mixing of the precursors.[25–27] In the case of PAO, mullite precursors mixture consists of stable α-Al_2O_3 with an average grain size of 1 μm and amorphous silica, yielded by the polymer, that coexist without any reaction up to 1250°C. Prior to the initial mullite formation (1400°C), the amorphous SiO_2 crystallizes into cristobalite between 1250 and 1350°C. At a temperature above 1400°C the successive reaction of the cristobalite with α-Al_2O_3 is thought to result in the formation of mullite partly via solid-state reactions at the newly formed α-Al_2O_3/cristobalite interfaces and partly through dissolution-precipitation reactions occurring in the coexisting aluminosilicate liquid phase. The high mullitization temperature is characteristic of an inhomogeneous mixture. Moreover, in the case of PAO a small amount of residual α-Al_2O_3 phase was retained in this sample, even though the sintering temperature was elevated to 1550°C. Because the mixing method used could not form a uniform mixture of SiO_2 and Al_2O_3 precursor powders, such residual phases including glassy phase, resulting from the eutectic in the SiO_2/Al_2O_3 system, remained in the sintered powders. On the other hand, in the PA and PAAO systems, in addition to α-Al_2O_3 and the amorphous silica, the mullite precursors mixture includes transition alumina yielded by Al oxidation. The beginning of mullite formation was achieved at lower temperatures (1200–1250°C). This indicates, like for diphasic aluminosilicate precursors, that the mixing scale of precursors was finer than in the PAO one. The lower temperature of mullitization and the presence of transition alumina may be indicative of a dual mechanism of mullitization. The first one is the mullite formation reaction, directly from the dissolution of transitional Al_2O_3 species into the coexisting glassy silica phase until the critical Al_2O_3 concentration is reached for mullite nucleation. The second one is the mullitization reaction via the individual crystallization of α-Al_2O_3 and cristobalite as in the case of PAO.

3.3. Sintering of green compacts

The dimensional changes associated with the reaction processes are shown in Fig. 6. Up to 400°C, all the mixtures expand (linear dilatation: 1–1.5%), followed up to 700°C by a subsequent shrinkage of about 3–3.5% that is primarily caused by the thermal degradation/

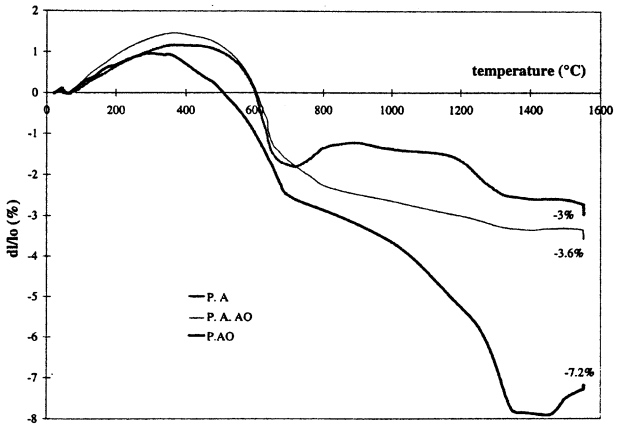

Fig. 6. Relative linear shrinkage of PAO, PA and PAAO compositions during oxidation and sintering under air.

oxidation of the polymer for the PAO sample. For the PA and PAAO ones, the evolution of this stage is modified by the oxidation of Al at low temperature.

In the case of siloxane/Al_2O_3 system, notable densification is observed for temperatures above about 1000°C, although shrinkage starts at a temperature higher than 800°C, and extends to the temperature at which mullitization starts (1350–1400°C). The final linear shrinkage of 7.2% corresponds to a pore volume of 18%.

The polymer/aluminium mixture presents a different dimensional behaviour. A transition stage for dimensional changes can be identified between 600 and 800°C, with a corresponding compensation of the shrinkage due to pyrolysis of the polymer by the volume expansion due to oxidation of Al. In the temperature range 800–1200°C the weak shrinkage of the compound corresponds to a similar behaviour that the one observed in the case of reaction-bonded aluminium oxide.[7] Moreover, the slight bow at 1000°C may indicate the onset of the transformation of the transition alumina to α-Al_2O_3. For a pore volume of 30%, the final linear shrinkage is 3%.

In the case of the PAAO mixture, after the pyrolysis stage, there is no significant dimension change. Only a continuous shrinkage of about 1.5% is observed from 700 to 1300°C. Here, the dilatation associated with the oxidation of Al is not sufficient to compensate the shrinkage due to the sintering of amorphous SiO_2 with α-Al_2O_3. Finally the total linear shrinkage, for a final pore volume of 20%, is 3.6%

In the whole of the materials, most sintering takes place by the viscous flow of the glassy silica phase, a mechanism which has been already proposed for the sintering of microcomposite powders of α-Al_2O_3 particles with glassy SiO_2.[28–31] Therefore, densification starts above about 1000–1050°C, beyond the softening temperature of the SiO_2-rich aluminosilicate glass, and occurs prior to mullitization. XRD patterns show that no reaction takes place within the temperature range 1000–1200°C

and that, during the corresponding densification, the glassy SiO_2-rich viscous phase is present. Due to the crystallization of the glassy SiO_2 into cristobalite at temperatures above 1200°C, the hindrance of the viscous flow is expected to result in the decrease of the shrinking rate.[28,32,33] For PAO, the period for mullitization can be identified beyond 1350°C, with a corresponding shrinkage compensation up to 1550°C caused by the volume expansion due to mullitization (+4.6 vol.%). For the PA and PAAO composites, mullitization proceeds at a lower temperature, with a consecutive liquid-phase sintering mechanism being dominant via the eutectic in α-Al_2O_3/SiO_2 system at about 1550°C.[23]

3.4. Microstructure

The results of Hg porosimetry are shown in Fig. 7. Two families of pores are evidenced for the whole of the mixtures: the first class is in the range 10–100 μm and the second one in the range 0.01–1 μm. It seems that the amount of the second class of pores increases with the amount of Al in the initial mixture and moreover there is a tendency for a bimodal pore size distribution centred at 0.2 and 0.6 μm respectively.

Fig. 8 shows the SEM micrographs of the representative microstructure of the PA and PAAO specimens. The observed morphological pore structure difference between the two samples confirms the results of the Hg porosimetry. The improvement obtained with the PAAO system can be seen by comparing the SEM micrographs, where large pores as those present in the PA specimen (Fig. 8a) have been replaced by a fine-distributed pore network (Fig. 8b). From the defect point of view the PAAO mixture appears as a good system because it presents minimum macroporosity and medium microporosity.

The typical TEM microstructures of PAO, PA and PAAO specimens sintered at 1550°C are shown in Figs. 9–11. The formation of nearly 3/2 mullite matrix grains was confirmed by EDS. The composition of the mullite is not constant through the PAO matrix and presents a small excess of Al_2O_3 (molar ratio of Al/Si in the range 3.14–3.24). For the PA and PAAO systems, the mullite matrix appears as rather homogeneous in composition and slightly Si-rich (Al/Si = 2.96).

The mullite matrix consisted of equiaxed grains, and not acicular-shaped grains, of about 1 μm in size. The granular-shaped mullite has been often correlated to the existence of residual glassy phase in the grain boundaries.[34,35] The occurrence of a thin glassy film (about 1nm in thickness), along certain grain boundaries was nevertheless confirmed by lattice fringe imaging (Fig. 12). However, HRTEM-images of some grain boundaries showed also clean and glass free interfaces where the lattice fringes of two mullite grains meet each other. This situation is not unique in mullite since, studying the glassy phase in sol-gel derived mullite, Kleebe et al.[36] found wetted and non wetted grain boundaries. In the same way, Mizuno[37] also found boundaries free from intergranular glassy phase in the microstructure of sintered 3/2 mullite.

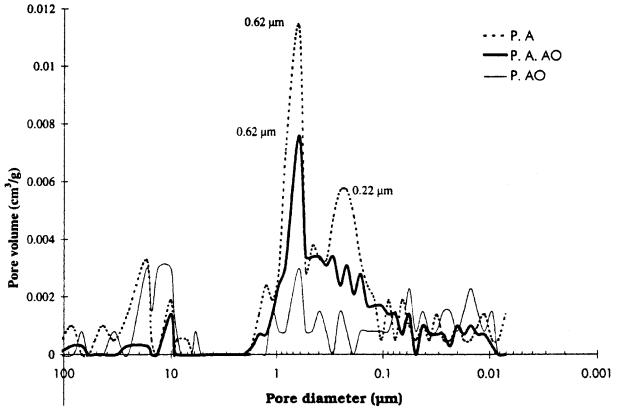

Fig. 7. Comparison of pore diameter for the three compositions.

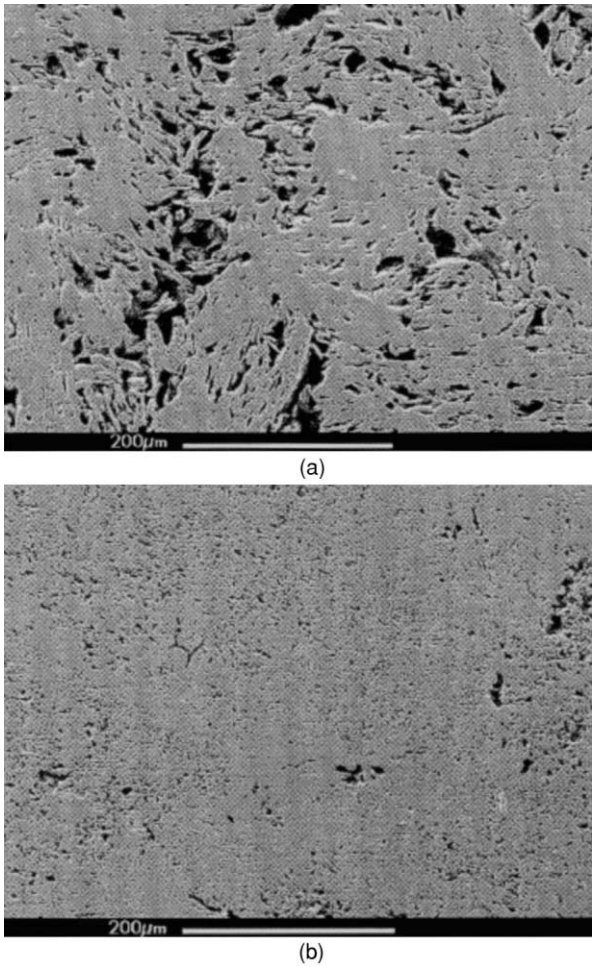

Fig. 8. SEM microstructures of PA (a) and PAAO (b) samples (scale bar = 200 μm).

Fig. 9. TEM microstructure of PAO sample (scale bar = 1 μm).

Some other specific microstructural features were encountered in the PAO samples. First, the mullite grains obtained from the PAO system contained a large amount of dislocations whereas grains in PA and PAAO samples were primarily dislocation free. Such high dislocation densities have been already observed elsewhere[18,19] and seem to be a characteristic in siloxane/Al_2O_3 derived mullites. It has been thought that a possible origin of the formation of a high defective mullite crystal structure may be the presence of oxycarbides in the aluminium-oxygen-carbon system, if carbon from the polymer precursor is not completely eliminated during oxidation.[18,19] In our case, these dislocations were not observed in the mullite structure derived from the polymer/Al system in which the presence of oxycarbides is not less probable than in the polymer/Al_2O_3 one. Thus, it is possible that the origin of these dislocations can be correlated to solid-state reactions due to the starting materials used to provide the Al_2O_3 species for the desired 3/2 mullite composition. In the PAO system the starting material was stable α-Al_2O_3 necessitating a relatively high energy to break its bonds to provide Al_2O_3 molecules. In the PA system, the starting material was oxidized Al giving transient alumina e.g. γ, θ and δ-Al_2O_3, that partly reacted with silica to form mullite nuclei and partly converted to α-Al_2O_3 before

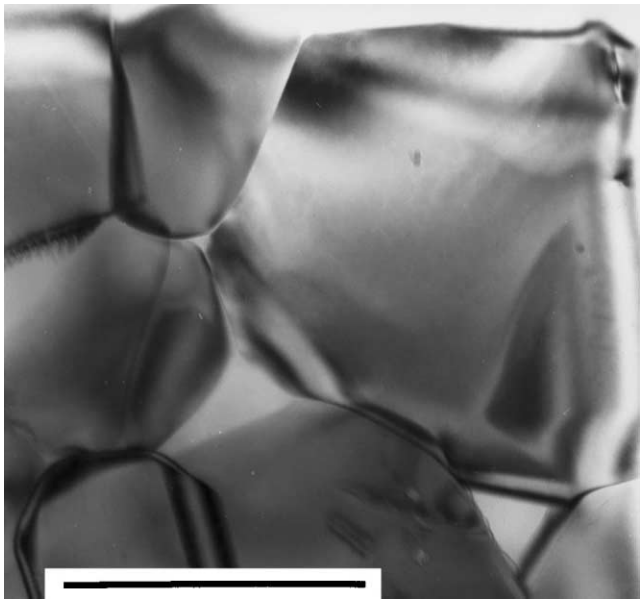

Fig. 10. TEM microstructure of PA sample (scale bar = 1 μm).

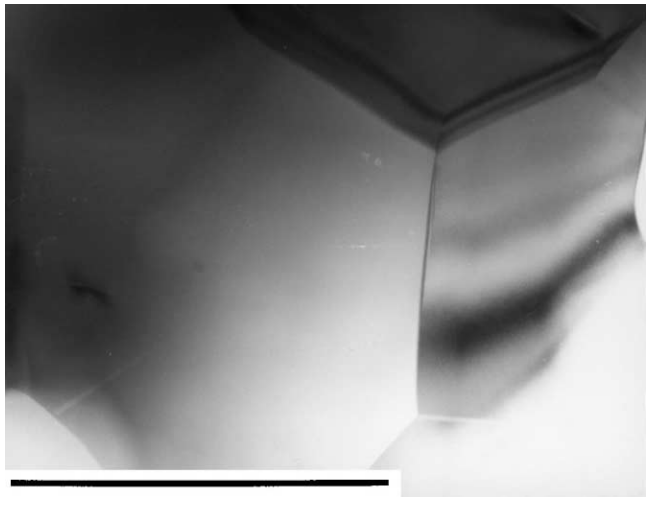

Fig. 11. TEM microstructure of PAAO sample (scale bar = 1 μm).

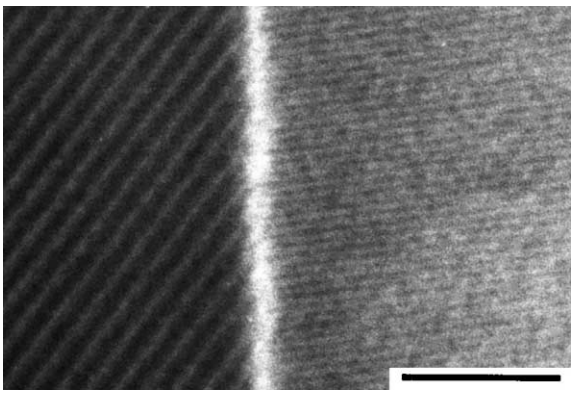

Fig. 12. HRTEM image of two mullite grains and the grain-boundary hinting at the appearance of a glassy phase (scale bar = 5 nm).

final transformation. On this basis, the use of α-Al_2O_3 seems to make restructuring more difficult and less perfect than the use of Al as the source of Al_2O_3.

In addition to dislocations, some particles, the apparent size of which is in the range 100–600 nm, are observed inside the mullite grains of the PAO system. From the results of EDS microanalysis, these particles are identified either as pure Al_2O_3 or as Al_2O_3 where Si^{4+} can substitute Al^{3+}. The largest Al_2O_3 particles (Fig. 13), with almost unchanged morphology, were coated with an Al-rich (Al/Si = 5.27) thin residual amorphous layer (d = 7 nm). However, micro-analysing by ATEM the tiny Al_2O_3-based particles (less than about 200 nm in apparent size) as well as the amorphous coating raises an experimental difficulty in the analyzed regions. In these regions, the specimen thickness is in the range 30–70 nm and when there is a portion of an alumina-based particle superimposed on a part of a mullite grain in the foil, the raw composition can correspond to a mixture of chemical compositions of several phases. The rounded shape of the smallest Al_2O_3-particles (Fig. 14) is a possible indication of the solution of Al_2O_3 in the surrounding material below a critical size of the residual alumina particles.[38]

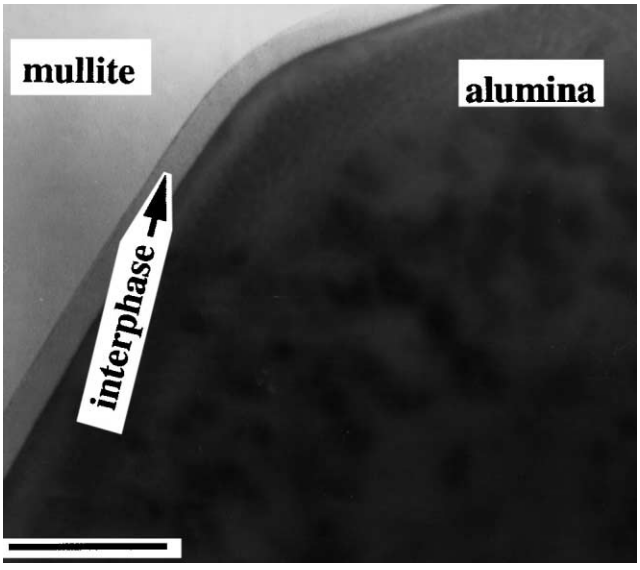

Fig. 13. Close-up of an alumina/mullite interphase showing the presence of an amorphous phase at the interphase (scale bar = 40 nm).

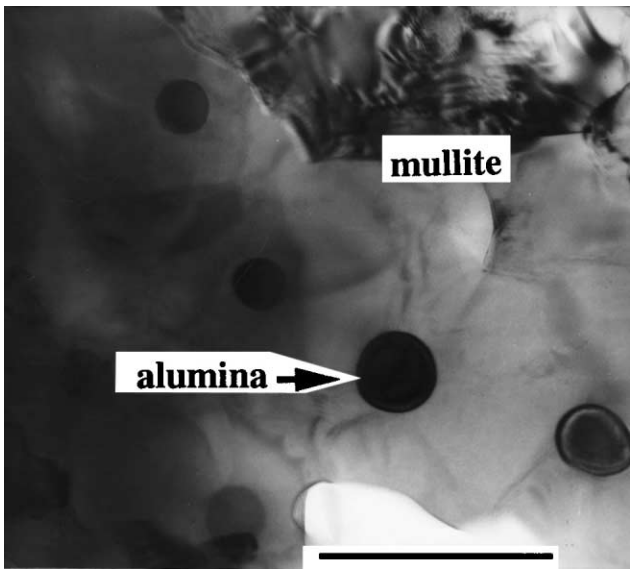

Fig. 14. TEM micrograph showing alumina particles inside mullite grains in PAO sample (scale bar = 1 μm).

3.5. Glassy phase pockets

The presence of small amounts of residual glassy phase located among mullite grains was commonly observed as glassy pockets at triple-junctions in the whole of the materials, which is consistent with that is expected for mullite materials sintered at a temperature (1550°C) near the eutectic one (1570 + /−20°C) in the SiO_2–Al_2O_3 system.[23]

The mean composition of the glassy phase pockets in the PAO sample is 10.5 mol% Al_2O_3, 87 mol% SiO_2 with about 2.5 mol% of impurities as $Na_2O + K_2O + MgO$. It is 6.5 mol% Al_2O_3, 93 mol% SiO_2 for the PA and the PAAO mixtures with a very small quantity (about 0.5 mol%) of $Na_2O + K_2O$ for the former system, and $Na_2O + K_2O + MgO$ for the latter. This mean composition of the glassy phase is in good accordance with results obtained by Kleebe et al.[36] and Thalcec et al.[39] They found about 10 mol% of Al_2O_3 and between about 6 and 12 mol% of Al_2O_3 content in SiO_2-glassy phase pockets respectively. Moreover, for the PA mixture, the composition of the glassy phase pockets is very near the eutectic composition (5 mol% of Al_2O_3) in the binary SiO_2–Al_2O_3 system.[23]

Some impurities like alkaline oxides can form liquids at temperatures lower than the eutectic temperature in the SiO_2–Al_2O_3 system. Furthermore, small amounts of alkaline impurities, as glass modifier, greatly change not

only the viscosity of glassy phases[40] but, certainly, their wetting characteristics. Effectively, as EDS analysis revealed, alkaline impurities (Na, K) were essentially concentrated in the glassy pockets observed at triple points. Finally, although mullite itself can incorporate about 0.5 wt.% MgO,[33] the presence of such a glass modifier, decreasing the viscosity of SiO_2-based glassy phase, should not be neglected in the sintering of the PAO and PAAO systems.

4. Conclusions

The active filler controlled pyrolysis of polymers has been used to synthesize 3/2 mullite from Al_2O_3-filled polydimethylsiloxane (PAO). This mullite has been compared to 3/2 mullite synthesized in the same conditions, with relatively low linear shrinkage, from Al-filled and Al/Al_2O_3-filled siloxanes (PA and PAAO systems respectively).

Due to a finer scale of mixing of the mullite precursors provided from active Al filler, the temperature of mullitization was lowered of about 150–200°C in the PAAO and PA systems.

In the PAO system, when α-Al_2O_3 was the only source of alumina, the equiaxed grains contained a large amount of dislocations. In PA and PAAO samples, transient Al_2O_3 making crystal reconstruction less difficult and more perfect, the grains were primarily dislocation free.

The presence of small amounts of residual glassy phase was observed as glassy pockets at triple-junctions in the whole of the materials. Their composition was near the eutectic one in the binary SiO_2–Al_2O_3 system.

The improved microstructure obtained with the PAAO mixture indicates that this ternary system seems to be the best compromise, for low shrinkage and low defect 3/2 mullite, between mullite obtained from Al-filled and Al_2O_3-filled siloxanes.

References

1. Parlier, M. and Colomban, P., Composites à matrice céramique pour applications thermostructurales. *La Recherche Aérospatiale*, 1996, **5-6**, 457–469.
2. Hyde, A. R., Ceramic matrix composites: high performance materials for space application. In *Proceeding of the International Symposium on Advanced Materials for Lightweight Structures*, ed. E.S.A., Noordwijk. 1992, pp. 255-260.
3. Warren, R. and Deng, S., Continuous fibre reinforced ceramic composites for very high temperatures. *Silicates Industriels*, 1995, **5-6**, 99–107.
4. Lundberg, R. and Eckerbom, L., Design and processing of all-oxide composites. *Ceram. Trans.*, 1995, **58**, 95–104.
5. Claussen, N., Le, T. and Wu, S., Low-shrinkage reaction-bonded alumina. *J. Eur. Ceram. Soc.*, 1989, **5**, 29–35.
6. Claussen, N., Processing, reaction mechanisms and properties of oxidation-formed Al_2O_3 matrix composites. *Journal de Physique IV-C7*, 1993, **3**, 1327–1334.
7. Wu, S., Holz, D. and Claussen, N., Mechanisms and kinetics of reaction-bonded aluminium oxide ceramics. *J. Am. Ceram. Soc.*, 1993, **76**(4), 970–980.
8. Holz, D., Wu, S., Scheppokat, S. and Claussen, N., Effect of parameters on phase and microstructure evolution in RBAO ceramics. *J. Am. Ceram. Soc.*, 1994, **77**(10), 2509–2517.
9. Claussen, N., Wu, S. and Holz, D., Reaction bonding of aluminium oxide (RBAO) composites: processing, reaction mechanisms and properties. *J. Eur. Ceram. Soc.*, 1994, **14**, 97–109.
10. Yajima, S., Hayashi, J., Omori, M. and Okamura, K., Development of a silicon carbide fibre with high tensile strength. *Nature*, 1976, **261**, 683–686.
11. Rice, R. W., Ceramics from polymer pyrolysis, opportunities and needs: a material perspective. *Ceram. Bull.*, 1983, **62**(8), 889–892.
12. Wills, R. R., Markle, R. A. and Mukhejee, S. P., Siloxanes, silanes, and silazanes in the preparation of ceramics and glasses. *Ceram. Bull.*, 1983, **62**(8), 904–911.
13. Wynne, K. J. and Rice, R. W., Ceramics via polymer pyrolysis. *Ann. Rev. Mater. Sci.*, 1984, **14**, 297–334.
14. Greil, P., Seibold, M. and Erny, T., Microcrystalline ceramic composites by active filler controlled reaction pyrolysis of polymers. *Mater. Res. Soc. Symp. Proc.*, 1992, **274**, 155–166.
15. Erny, T., Seibold, M., Jarchow, O. and Greil, P., Microstructure development of oxycarbide composites during active-filler-controlled polymer pyrolysis. *J. Am. Ceram. Soc.*, 1993, **76**(1), 207–213.
16. Greil, P., Active-filler-controlled pyrolysis of preceramic polymers. *J. Am. Ceram. Soc.*, 1995, **78**(4), 835–848.
17. Walter, S., Suttor, D., Erny, T., Hahn, B. and Greil, P., Injection moulding of polysiloxane/filler mixtures for oxycarbide ceramic composites. *J. Eur. Ceram. Soc.*, 1996, **16**, 387–393.
18. Suttor, D., Kleebe, H. J. and Ziegler, G., Synthetic low-shrinkage oxide-matrices from filled polymeric siloxanes. *Ceram. Eng. Sci. Proc.*, 1997, **17**(4), 27–35.
19. Suttor, D., Kleebe, H. J. and Ziegler, G., Formation of mullite from filled siloxanes. *J. Am. Ceram. Soc.*, 1997, **80**(10), 2541–2548.
20. Suttor, D., Kleebe, H. J. and Ziegler, G., Low-shrinkage mullite derived from filled polymeric siloxanes. *Key Eng. Mater.*, 1997, **132-136**, 448–451.
21. Thomas, T. H. and Kendrick, T. C., Thermal analysis of poly(-dimethylsiloxanes). I: Thermal degradation in controlled atmospheres. *J. Poly. Sci.*, 1969, **A2**(7), 537–549.
22. Ring, T. A., *Fundamentals of Ceramic Powder Processing and Synthesis*. Academic Press, 1996.
23. Pask, J. A., Importance of starting materials on reactions and phase equilibria in the α-Al_2O_3–SiO_2 system. *J. Eur. Ceram. Soc.*, 1996, **16**, 101–108.
24. Kara, F. and Little, J. A., Sintering behavior of precursors of mullite powders and resultant microstructures. *J. Eur. Ceram. Soc.*, 1996, **16**(6), 627–635.
25. Wu, S., Holz, D. and Claussen, N., Mechanisms and kinetics of reaction-bonded aluminium oxide ceramics. *J. Am. Ceram. Soc.*, 1993, **76**(4), 970–980.
26. Pask, J. A. and Tompsia, A. P., Formation of mullite from sol-gel mixtures and kaolinite. *J. Am. Ceram. Soc.*, 1975, **58**(11-12), 507–512.
27. Okada, K. and Otsuka, N., Formation process of mullite. In *Ceramic Transactions, Vol 6, Mullite and Mullite Matrix Composites*, ed. S. Somiya, R. F. Davis and J. A. Pask. American Ceramic Society, Westerville, 1990, pp. 357–387.
28. Schneider, H., Saruhan, B., Voll, D., Merwin, L. and Sebald, A., Mullite precursor phases. *J. Eur. Ceram. Soc.*, 1993, **11**, 87–94.
29. Nurishi, Y. and Pask, J. A., Sintering of α-Al_2O_3/amorphous silica compact. *Ceram. Int.*, 1982, **8**, 57–59.
30. Rana, A. P. S., Aiko, O. and Pask, J. A., Sintering of α-Al_2O_3/quartz and α-Al_2O_3/cristobalite related to mullite formation. *Ceram. Int.*, 1982, **8**, 151–153.

31. Sacks, M. D., Bozkurt, N. and Scheiffele, G. W., Fabrication of mullite and mullite-matrix composites by transient viscous sintering of composite powders. *J. Am. Ceram. Soc.*, 1991, **74**(10), 2428–2437.
32. Rodrigo, P. D. D. and Boch, P., High purity mullite ceramics by reaction sintering. *Int. J. High. Technol. Ceram.*, 1985, **1**, 3–30.
33. Schneider, H., Okada, K. and Pask, J. A., *Mullite and Mullite Ceramics*, ed. H. Schneider, K. Okada and J. A. Pask, John Wiley & Sons, Chichester, 1994.
34. Pask, J. A., Zhag, X. W., Tomsia, A. P. and Yoldas, B. E., Effect of sol-gel mixing on mullite microstructure and phase equilibria in the α-Al_2O_3–SiO_2 system. *J. Am. Ceram. Soc.*, 1987, **70**(10), 704–707.
35. Ismail, M. G. M. U., Nakai, Z. and Somiya, S., Microstructure and mechanical properties of mullite prepared by the sol-gel method. *J. Am. Ceram. Soc.*, 1987, **70**(1), C7–8.
36. Kleebe, H. J., Hiltz, G. and Ziegler, G., Transmission electron microscopy and electron energy-loss spectroscopy characterization of glass phase in sol-gel derived mullite. *J. Am. Ceram. Soc.*, 1996, **79**(10), 2592–2600.
37. Mizumo, M., Microstructure, microchemistry, and flexural strength of mullite ceramics. *J. Am. Ceram. Soc.*, 1991, **74**(10), 3017–3022.
38. Kleebe, H. J., Siegelin, F. and Ziegler, G., Stable versus metastable formation mechanism of mullite studied by transmission electron microscopy. In: *British Ceramic Proceedings, Vol 60*, *Extended Abstracts of the Sixth Conference & Exhibition of the European Ceramic Society*. IOM Communications Ltd, London, 1999, pp. 87–88.
39. Thalcec, E., Nass, R., Krajewski, T., Rein, R. and Schmidt, H., Microstructure and mechanical properties of slip cast sol-gel derived mullite. *J. Eur. Ceram. Soc.*, 1998, **18**, 1089–1099.
40. Zarzycki, J., *Les Verres et l'état Vitreux*. Masson, Paris, 1982, pp. 226–227.